

Synergistic Effects of TiO₂ and Palladium-Based Cocatalysts on the Selective Oxidation of Ethene to Acetic Acid on Mo–V–Nb Oxide Domains**

Xuebing Li and Enrique Iglesia*

Methanol carbonylation on Rh and Ir organometallic complexes with iodide co-catalysts is currently used to produce acetic acid.^[1] Catalyst cost and recovery, as well as the toxic and corrosive nature of iodide compounds, has led a search for alternate routes, such as zeolite acid catalysts for methanol^[2] or dimethyl ether^[3] carbonylation and dispersed metal oxide domains for the oxidation of ethane,^[4] ethene,^[5] and ethanol.^[6] A commercial process using Pd-promoted (1.5 % wt. Pd) heteropolyacid (HPA) catalysts for ethene oxidation was reported to give approximately 80 % acetic acid selectivities at low temperatures (ca. 420 K).^[5] These polyoxometalate clusters, promoted with high concentrations of noble metals, are expensive and do not maintain their structure during the oxidative processes required for the regeneration of deactivated catalysts.^[7]

Mo–V oxides catalyze the (ammo)oxidation of alkanes^[8] and the oxidation of unsaturated molecules to carboxylic acids.^[9] Multicomponent oxides promoted by noble metals ($\text{Mo}_{0.396}\text{V}_{0.128}\text{Nb}_{0.128}\text{Pd}_{3.84 \times 10^{-4}}$) gave high acetic acid selectivities (ca. 80 %) using ethene as a reactant. Their high stability allowed their use as catalysts at relatively high temperatures (560 K), which led, in turn, to higher acetic acid productivities^[9d] than on polyoxometalate-based catalysts.

We have found that the presence of TiO₂ as a colloidal suspension during precipitation of Mo–V–Nb oxides leads to markedly higher rates for oxidation of ethane, ethene, and ethanol to acetic acid. We report herein these effects for ethene oxidation and provide evidence for the marked influence of Pd sites, present as trace components (0.0025–0.005 % wt.) within physical mixtures, on the rate of conversion of ethene into acetaldehyde, a rate-determining step in acetic acid synthesis.^[10] The catalytic materials reported herein catalyze ethene oxidation to acetic acid with much higher rates than on other catalysts, while using only trace amounts of costly Pd components. The ability of Pd promoters to act effectively within physical mixtures allows independent

optimization of the Pd and oxide functions and much more efficient use of costly noble metals.

Figure 1 shows ethene conversion rates and acetic acid selectivities on $\text{Mo}_{0.61}\text{V}_{0.31}\text{Nb}_{0.08}\text{O}_x$ and $\text{Mo}_{0.61}\text{V}_{0.31}\text{Nb}_{0.08}\text{O}_x/\text{TiO}_2$ catalysts. Both materials showed high initial acetic acid selectivities (70 %), which decreased with increasing ethene conversion, as a result of secondary oxidation of acetic acid to CO and CO₂ (CO_x). Catalysts prepared by precipitation of active oxides in the presence of a colloidal suspension of pre-formed TiO₂ (24 % $\text{Mo}_{0.61}\text{V}_{0.31}\text{Nb}_{0.08}\text{O}_x/\text{TiO}_2$) gave ethene oxidation rates approximately 10-times higher (per active component) and around 2.5-times higher (per mass) than powders with similar V–Mo–Nb composition (Figure 1a). The surface area of $\text{Mo}_{0.61}\text{V}_{0.31}\text{Nb}_{0.08}\text{O}_x/\text{TiO}_2$ is 34 m² g^{−1} (from N₂ physisorption at its normal boiling point), and approx-

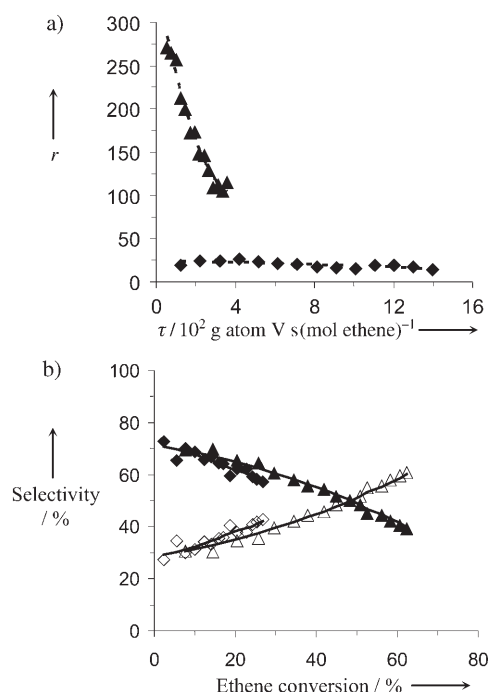


Figure 1. Catalytic oxidation of ethene at 573 K on $\text{Mo}_{0.61}\text{V}_{0.31}\text{Nb}_{0.08}\text{O}_x$ and $\text{Mo}_{0.61}\text{V}_{0.31}\text{Nb}_{0.08}\text{O}_x/\text{TiO}_2$. a) ethene conversion rate r (in $10^{-5} \text{ mol (g atom V)}^{-1} \text{ s}^{-1}$) on $\text{Mo}_{0.61}\text{V}_{0.31}\text{Nb}_{0.08}\text{O}_x$ (♦) and $\text{Mo}_{0.61}\text{V}_{0.31}\text{Nb}_{0.08}\text{O}_x/\text{TiO}_2$ (▲) against residence time τ . b) Selectivity of acetic acid (full symbols) and CO_x (open symbols) on $\text{Mo}_{0.61}\text{V}_{0.31}\text{Nb}_{0.08}\text{O}_x$ (acetic acid (♦), CO_x (◇)) and on $\text{Mo}_{0.61}\text{V}_{0.31}\text{Nb}_{0.08}\text{O}_x/\text{TiO}_2$ (acetic acid (▲) and CO_x (△)); solid lines (—): predicted selectivities from Equation (1). Partial pressures [kPa]: ethene 32, O₂ 107, H₂O 320, He 1130, N₂ 11.

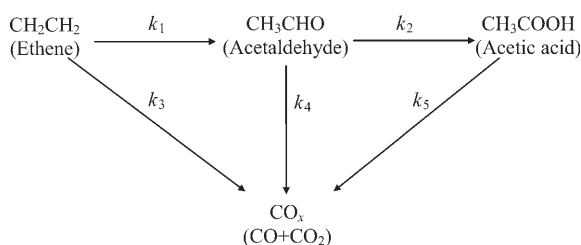
[*] Dr. X. Li, Prof. E. Iglesia
Department of Chemical Engineering
University of California at Berkeley
Berkeley, CA 94720 (USA)
Fax: (+1) 510-642-4778
E-mail: iglesias@berkeley.edu

[**] The financial support of ExxonMobil Research and Engineering Co. is gratefully acknowledged.

Supporting information for this article is available on the WWW under <http://www.angewandte.org> or from the author.

imately 80% of the TiO₂ surface is covered by active components (from CO₂ chemisorption at 313 K). These data indicate that active Mo–V–Nb oxide has an area of about 28 m² g^{−1}, which is approximately 3-times higher than for bulk Mo_{0.61}V_{0.31}Nb_{0.08}O_x powders (7.8 m² g^{−1}). Areal ethene oxidation rates are similar on Mo_{0.61}V_{0.31}Nb_{0.08}O_x/TiO₂ (6.9 × 10^{−8} mol s^{−1} m^{−2}) and Mo_{0.61}V_{0.31}Nb_{0.08}O_x (8.3 × 10^{−8} mol s^{−1} m^{−2}). The higher rates reported for TiO₂-supported samples reflect a higher dispersion of active Mo–V–Nb structures, without significant effects of dispersion on their intrinsic reactivity or selectivity, as also found for ethane and ethanol oxidation.^[6a,10] The marked decrease in ethene conversion rates on Mo_{0.61}V_{0.31}Nb_{0.08}O_x/TiO₂ with increasing residence time (τ) reflects the depletion of reactants at the higher conversions, resulting from the much higher reactivity of this catalyst relative to the bulk catalyst.

CO and CO₂ (CO_x) were the predominant side products on Mo_{0.61}V_{0.31}Nb_{0.08}O_x and Mo_{0.61}V_{0.31}Nb_{0.08}O_x/TiO₂; acetaldehyde formed with selectivities < 1% at all ethene conversions. CO_x selectivity increased with increasing conversion and reactor residence time (Figure 1b), but was significant (28%) even at near-zero conversion, indicating that CO_x formed by the direct oxidation of ethene and of acetaldehyde and acetic acid. These data indicate that ethene oxidation proceeds by oxidation to acetaldehyde and subsequent acetaldehyde oxidation to acetic acid (Scheme 1).



Scheme 1. Parallel sequential reaction pathways in ethene oxidation.

Assuming first-order dependencies on reactants and acetaldehyde intermediates at quasi-steady-state, the selectivity of acetic acid in plug-flow or batch reactors is given by Equations (1) and (2).

$$S_{\text{CH}_3\text{CHOOH}} = \frac{k_{\text{eff}}(e^{-(k_{\text{eff}}+k_3)P_{\text{CH}_2\text{CH}_2}^0\tau} - e^{-k_3P_{\text{CH}_2\text{CH}_2}^0\tau})}{(k_5 - (k_{\text{eff}} + k_3))(1 - e^{-(k_{\text{eff}}+k_3)P_{\text{CH}_2\text{CH}_2}^0\tau})} \quad (1)$$

$$k_{\text{eff}} = \frac{k_1}{1 + \frac{k_4}{k_2}} \cong k_1 \quad (2)$$

$P_{\text{CH}_2\text{CH}_2}^0$ is the inlet ethene pressure and τ (g atom Vs (mol ethene)^{−1}) is the residence time. A polynomial expansion to

order τ² gives Equation (3).

$$S_{\text{CH}_3\text{CHOOH}} = \frac{k_{\text{eff}}}{k_{\text{eff}} + k_3} \frac{1 - \frac{1}{2}(k_{\text{eff}} + k_3 + k_5)P_{\text{CH}_2\text{CH}_2}^0\tau}{1 - \frac{1}{2}(k_{\text{eff}} + k_3)P_{\text{CH}_2\text{CH}_2}^0\tau} \quad (3)$$

As τ → 0, the selectivity then becomes Equation (4).

$$S_{\text{CH}_3\text{CHOOH}}^0 = \frac{k_{\text{eff}}}{k_{\text{eff}} + k_3} \quad (4)$$

Thus, k_{eff} and k_3 can be measured from the ethene conversion rates and selectivities (as τ → 0), while k_5 is derived from the effects of τ on selectivities (Table 1). The k_{eff} values

Table 1: Rate constants for ethene oxidation on multicomponent metal oxide catalysts.^[a]

Catalyst	Rate constants ^[b]			Ratio	
	k_{eff}	k_3	k_5	k_{eff}/k_3	k_{eff}/k_5
Mo _{0.61} V _{0.31} Nb _{0.08} O _x	0.68	0.26	0.95	2.6	0.72
Mo _{0.61} V _{0.31} Nb _{0.08} O _x /TiO ₂	7.0	2.7	8.8	2.6	0.80
0.0025% Pd/Mo _{0.61} V _{0.31} Nb _{0.08} O _x /TiO ₂	140	22	7.0	6.5	3.1

[a] Reaction conditions: T = 573 K; P_{tot} = 1.6 MPa; Partial pressures [kPa]: ethene 32, O₂ 107, H₂O 320, He 1130, and N₂ 11. [b] Rate constants in [10^{−5} mol (g atom V)^{−1} s^{−1} kPa^{−1}].

are much larger on TiO₂-containing than on bulk catalysts, but k_{eff}/k_3 and k_{eff}/k_5 ratios are similar, confirming that TiO₂ present during precipitation of Mo_{0.61}V_{0.31}Nb_{0.08}O_x increased the number (higher k_{eff}) but not the type of active sites. Figure 1b also shows that the selectivities predicted by Equation (1) at various conversions are consistent with our experimental results.

The low acetaldehyde concentrations indicate that acetaldehyde reacts rapidly to form acetic acid and that ethene conversion into acetaldehyde limits the overall reaction rates. In light of this situation, we examined the use of palladium, a known catalyst for ethene oxidation,^[11] as part of a physical mixture to overcome these kinetic hurdles.

The sequential reaction pathways proposed in Scheme 1 do not require that the sites for ethene oxidation to acetaldehyde reside within molecular distances (defined as those required for a C₂ molecule to access the site in a concerted manner) of Mo_{0.61}V_{0.31}Nb_{0.08}O_x/TiO₂ sites active in acetaldehyde oxidation to acetic acid. We explored the addition of a Pd component in concentrations (0.0025–0.005% wt. based on physical mixture) 4–600-times lower than previously used (1.5% wt. ref. [5] and 0.02% wt. ref. [9d]) as physical mixtures of Mo_{0.61}V_{0.31}Nb_{0.08}O_x/TiO₂ and 0.3% wt. of Pd/SiO₂. Physical mixtures, in contrast to the addition of Pd salts to Mo_{0.61}V_{0.31}Nb_{0.08}O_x/TiO₂, allow independent variations of the two components, without disturbing the structure or dispersion of one by the presence of the other. This approach also prevents Pd incorporation into the inaccessible bulk of large Mo–V–Nb oxide crystallites, which occurred in previous studies.^[9a,d]

The presence of Pd (as low as 0.0025% wt.) led to more than a ten-fold increase in acetic acid synthesis rates (per active Mo–V–Nb component, rates from local derivatives of ethene concentration with respect to reaction time) relative to

palladium-free $\text{Mo}_{0.61}\text{V}_{0.31}\text{Nb}_{0.08}\text{O}_x/\text{TiO}_2$ (Figure 2a). Pd/SiO_2 also increased acetic acid selectivities (Figure 2b), even though ethene oxidation on Pd/SiO_2 by itself formed pre-

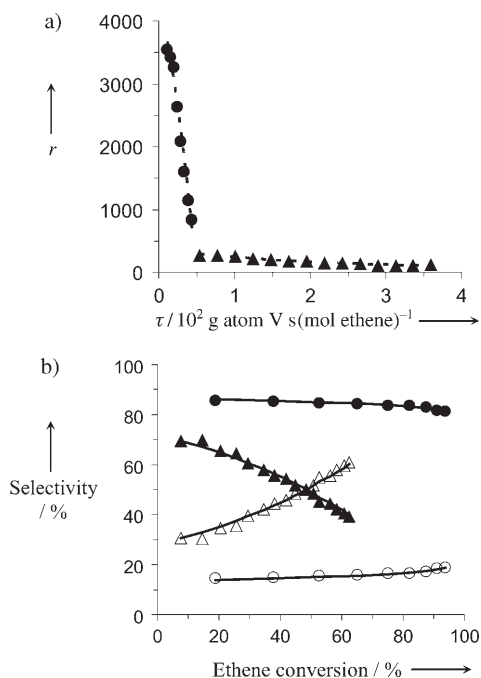


Figure 2. Catalytic oxidation of ethene at 573 K on $\text{Mo}_{0.61}\text{V}_{0.31}\text{Nb}_{0.08}\text{O}_x/\text{TiO}_2$ and $0.0025\% \text{ Pd}/\text{Mo}_{0.61}\text{V}_{0.31}\text{Nb}_{0.08}\text{O}_x/\text{TiO}_2$ prepared by physically mixing of $\text{Mo}_{0.61}\text{V}_{0.31}\text{Nb}_{0.08}\text{O}_x/\text{TiO}_2$ and $0.03\% \text{ Pd}/\text{SiO}_2$. a) ethene conversion rate r (in $10^{-5} \text{ mol (g atom V)}^{-1} \text{ s}^{-1}$) on $\text{Mo}_{0.61}\text{V}_{0.31}\text{Nb}_{0.08}\text{O}_x/\text{TiO}_2$ (▲) and $0.0025\% \text{ Pd}/\text{Mo}_{0.61}\text{V}_{0.31}\text{Nb}_{0.08}\text{O}_x/\text{TiO}_2$ (●); b) selectivity of acetic acid (full symbols) and CO_x (open symbols) on $\text{Mo}_{0.61}\text{V}_{0.31}\text{Nb}_{0.08}\text{O}_x/\text{TiO}_2$ (acetic acid (▲) and CO_x (△)) and on $0.0025\% \text{ Pd}/\text{Mo}_{0.61}\text{V}_{0.31}\text{Nb}_{0.08}\text{O}_x/\text{TiO}_2$ (acetic acid (●) and CO_x (○)); solid lines (—): predicted selectivities from Equation (1). Partial pressures [kPa]: ethene 32, O_2 107, H_2O 320, He 1130, N_2 11.

dominantly CO_x (80% CO_x at 3–12% ethene conversion at the conditions of Figure 1 and Figure 2). These data show that acetaldehyde is rapidly oxidized to CO_x on PdO_x , unless it is scavenged by oxidation to acetic acid on $\text{Mo}_{0.61}\text{V}_{0.31}\text{Nb}_{0.08}\text{O}_x$. The k_{eff} values on palladium-containing mixtures (0.0025% wt.) were approximately 20-fold higher than on $\text{Mo}_{0.61}\text{V}_{0.31}\text{Nb}_{0.08}\text{O}_x/\text{TiO}_2$, but ethene combustion (k_3) rate constants increased by only a factor of about 8 and acetic acid combustion rate constants (k_5) were essentially unaffected by Pd (Table 1). These effects led to much higher k_{eff}/k_3 and k_{eff}/k_5 rate constant ratios on palladium-containing mixtures and to markedly higher acetic acid

selectivities. Selectivities predicted by Equation (1) at various ethene conversions are also shown for palladium-promoted $\text{Mo}_{0.61}\text{V}_{0.31}\text{Nb}_{0.08}\text{O}_x/\text{TiO}_2$ in Figure 2b (solid lines).

We conclude that PdO_x sites are not directly involved in acetic acid formation (step 2 of the sequential reaction pathway), but merely form acetaldehyde intermediates (step 1), which would convert into CO_x without the presence of $\text{Mo}_{0.61}\text{V}_{0.31}\text{Nb}_{0.08}\text{O}_x$ sites that scavenge acetaldehyde to form acetic acid. Acetic acid is a much less reactive molecule in subsequent oxidation reactions, as expected from the respective energies of the weakest C–H bond in acetic acid ($\text{H}-\text{CH}_2\text{C}(\text{O})\text{OH}$, $398.7 \text{ kJ mol}^{-1}$) and acetaldehyde ($\text{CH}_3\text{C}(\text{O})-\text{H}$, 374 kJ mol^{-1}).^[12,13]

An increase in ethene pressure or Pd content increased acetic acid synthesis rates (Table 2). Acetic acid synthesis rates increased from 4.5 to $16.4 \text{ g acetic acid (g catalyst)}^{-1} \text{ cat h}^{-1}$ on $0.0025\% \text{ Pd}/\text{Mo}_{0.61}\text{V}_{0.31}\text{Nb}_{0.08}\text{O}_x/\text{TiO}_2$ as the ethene pressure increased from 32 to 533 kPa. The weaker than linear increase in rate with pressure may reflect kinetically relevant re-oxidation steps in the redox cycle, as a result of the high pressure and reactive nature of ethene reactants. Rates increased from 16.4 to $28.0 \text{ g acetic acid (g catalyst)}^{-1} \text{ h}^{-1}$ as the Pd content increased from 0.0025% wt. to 0.005% wt. These rates are much higher than those on previously reported catalysts (Table 2).^[5,9d] Acetaldehyde selectivities increased with ethene pressure, because its conversion into acetic acid was less affected by ethene pressure than its formation rate.

Palladium-promoted multicomponent metal oxides show unprecedented reactivity in ethene oxidation to acetic acid. Precipitation of Mo–V–Nb active oxides in the presence of colloidal TiO_2 led to much higher active surface areas than in unsupported oxides. Palladium increased the rate of ethene oxidation to acetaldehyde, while active Mo–V–Nb oxides rapidly oxidized the acetaldehyde intermediates to stable acetic acid products, thus preventing acetaldehyde combustion pathways prevalent on monofunctional palladium-based catalysts. These synergistic bifunctional effects are evident even in physical mixtures, thus allowing independent optimization of the two catalytic functions.

Table 2: Catalytic oxidation of ethene to acetic acid.

Catalyst	T [K]	Ethene P [kPa]	Ethene conv. [%]	Acetaldehyde	Selectivity [%] Acetic acid	CO_x	Prod. ^[a]
$0.0025\% \text{ Pd}/\text{Mo}_{0.61}\text{V}_{0.31}\text{Nb}_{0.08}\text{O}_x/\text{TiO}_2$ ^[b]	575	32	21.1	trace	89	11	4.5
$0.0025\% \text{ Pd}/\text{Mo}_{0.61}\text{V}_{0.31}\text{Nb}_{0.08}\text{O}_x/\text{TiO}_2$ ^[b]	577	533	6.4	13	63	24	16.4
$0.005\% \text{ Pd}/\text{Mo}_{0.61}\text{V}_{0.31}\text{Nb}_{0.08}\text{O}_x/\text{TiO}_2$ ^[b]	594	533	5.5	17	64	19	28.0
$\text{Pd}-\text{Se}(0.02)-\text{H}_4\text{SiW}_{12}\text{O}_{40}$ ^[c]	423	245	6	87	8	5	0.24
$\text{Mo}_{1.0}\text{V}_{0.396}\text{Nb}_{0.128}\text{Pd}_{3.84}\times 10^{-4}$ ^[d]	558	190	63	trace	78	22	1.30

[a] Productivity [in $\text{g acetic acid (g catalyst)}^{-1} \text{ h}^{-1}$]. [b] Reaction conditions: P_{tot} : 1.6 MPa; partial pressure [kPa]: ethene 32 or 533, O_2 107, H_2O 320, He 1130, and N_2 11. [c] Ref. [5], P_{tot} : 0.49 MPa; partial pressure [kPa]: ethene 245, O_2 34, H_2O 147, and N_2 64. [d] Ref. [9d], P_{tot} : 1.4 MPa; partial pressure [kPa]: ethene 190, air 1080, and H_2O 130.

Experimental Section

$\text{Mo}_{0.61}\text{V}_{0.31}\text{Nb}_{0.08}\text{O}_x$ powders were prepared using a slurry method reported previously.^[4] A $\text{C}_4\text{O}_8\text{NbOH}\cdot\text{NH}_3$ (Aldrich; 99.99 %) solution was added at ambient temperature to a stirred solution containing $\text{C}_2\text{O}_4\text{H}_2$ (Fluka, 99 %), NH_4VO_3 (Sigma-Aldrich, 99 %), and $(\text{NH}_4)_6\text{Mo}_7\text{O}_{24}\cdot 4\text{H}_2\text{O}$ (Aldrich, 99.98 %). Water was evaporated while stirring under dynamic vacuum at 363 K. The powders formed were dried in ambient air overnight at 393 K and then treated in flowing dry air (Praxair, extra dry, $1.67\text{ cm}^3\text{ s}^{-1}$) at 673 K for 4 h. In the preparation of the $\text{Mo}_{0.61}\text{V}_{0.31}\text{Nb}_{0.08}\text{O}_x/\text{TiO}_2$ (24 % wt.) the TiO_2 (Degussa, P25, BET: $50\text{ m}^2\text{ g}^{-1}$, anatase/rutile = 3:1) was introduced into the starting solution before adding the $\text{C}_4\text{O}_8\text{NbOH}\cdot\text{NH}_3$ solution.

Ethene oxidation rates and selectivities were measured at 1.6 MPa and 573 K with C_2H_4 (32 or 533 kPa, Praxair, 99.95 %), O_2/N_2 (118 kPa, Praxair mixture, 10 % N_2 in O_2 , certified), H_2O (320 kPa, deionized), and He (as balance, Praxair, 99.999 %) as reactants. Kinetic studies were carried out in a high-pressure gradientless batch reactor (reactor content: 206 cm^3) held within an insulated box at a constant temperature (ca. 433 K) to avoid condensation. The reactor contents were recirculated at $20\text{ cm}^3(\text{STP})\text{ s}^{-1}$ using a graphite gear micropump. The effects of reactant pressures were examined using a single-pass flow reactor. A high-pressure syringe pump (Teledyne Isco Inc., model: 500D) was used to introduce H_2O (deionized) and the system was kept above 433 K to avoid condensation. Reactants and products were analyzed by online gas chromatography (HP 5890, II).

CO_2 chemisorption uptakes were measured with a Quantachrome 1C Autosorb unit by evacuating samples at 673 K and exposing samples to CO_2 (Praxair, 99.998 %) at 313 K. CO_2 uptakes were calculated by extrapolation of uptakes to zero pressure.

Received: February 9, 2007

Revised: April 30, 2007

Published online: October 9, 2007

Keywords: acetic acid · ethene · heterogeneous catalysis · metal oxides · oxidation

- [1] a) F. E. Paulik, J. F. Roth, *Chem. Commun.* **1968**, 1578a–1578a; b) G. J. Sunley, D. J. Watson, *Catal. Today* **2000**, 58, 293–307.
- [2] W. J. Smith (BP Chemicals Limited), US 5420345, **1995**.
- [3] P. Cheung, A. Bhan, G. J. Sunley, E. Iglesia, *Angew. Chem.* **2006**, 118, 1647–1650; *Angew. Chem. Int. Ed.* **2006**, 45, 1617–1620.
- [4] E. M. Thorsteinson, T. P. Wilson, F. G. Young, P. H. Kasai, *J. Catal.* **1978**, 52, 116–132.
- [5] K. I. Sano, H. Uchida, S. Wakabayashi, *Catal. Surv. Jpn.* **1999**, 3, 55–60.
- [6] a) X. Li, E. Iglesia, *Chem. Eur. J.*, in press; b) K. Yamaguchi, N. Mizuno, *Angew. Chem.* **2002**, 114, 4720–4724; *Angew. Chem. Int. Ed.* **2002**, 41, 4538–4542; c) C. H. Christensen, B. Jørgensen, J. Rass-Hansen, K. Egeblad, R. Madsen, S. K. Klitgaard, S. M. Hansen, M. R. Hansen, H. C. Andersen, A. Riisager, *Angew. Chem.* **2006**, 118, 4764–4767; *Angew. Chem. Int. Ed.* **2006**, 45, 4648–4651.
- [7] J. Melsheimer, S. S. Mahmoud, B. Mestl, R. Schlögl, *Catal. Lett.* **1999**, 60, 103–111.
- [8] M. M. Lin, *Appl. Catal. A* **2001**, 207, 1–16.
- [9] a) D. Linke, D. Wolf, M. Baerns, O. Timpe, R. Schlögl, S. Zeyß, U. Dingerdissen, *J. Catal.* **2002**, 205, 16–31; b) W. Ueda, D. Vitry, T. Katou, *Catal. Today* **2004**, 96, 235–240; c) B. Solsona, J. M. López Nieto, J. M. Oliver, J. P. Gumbau, *Catal. Today* **2004**, 91–92, 247–250; d) K. Karim, K. Sheikh, WO 200000284, **2000**.
- [10] X. Li, E. Iglesia, *Appl. Catal. A*, submitted.
- [11] J. Smidt, W. Hafner, R. Jira, J. Sedlmeier, R. Sieber, R. Rüttinger, H. Kojer, *Angew. Chem.* **1959**, 71, 176–182.
- [12] Y. R. Luo, J. A. Kerr, *Handbook of Chemistry and Physics*, CRC, Boca Raton, **2007**, p. 9–61.
- [13] a) C. Batiot, B. K. Hodnett, *Appl. Catal. A* **1996**, 137, 179–191; b) F. E. Cassidy, B. K. Hodnett, *CatTech* **1998**, 2, 173–180.